

IRON OXIDE PIGMENTING POWDERS PRODUCED BY THERMAL TREATMENT OF IRON SOLID WASTES FROM STEEL MILL PICKLING LINES*

C. Sikalidis^{1***}, T. Zorba², K. Chrissafis² and K. M. Paraskevopoulos²

¹Chemical Engineering Department, Aristotle University of Thessaloniki, 54124 Thessaloniki, Greece

²Physics Department, Aristotle University of Thessaloniki, 54124 Thessaloniki, Greece

Phase changes of iron containing solid wastes from steel mill pickling lines after thermal treatments were investigated aiming the determination of the appropriate conditions for its transformation to be useful for industrial raw materials. Above 275°C, the thermally treated wastes contain a mixture of $\alpha\text{-Fe}_2\text{O}_3$ (hematite) and $\gamma\text{-Fe}_2\text{O}_3$ (maghemite) in different proportions, depending on the maximum heating temperature of the thermal treatment. Increasing the maximum temperature the maghemite participation is decreased through its transformation to hematite. Above 850°C hematite is the main constituent, suggesting that thermal treatment of the wastes in this temperature will give a product that could be used as red iron pigment.

Keywords: hematite, FTIR, maghemite, steel mill wastes, TG-DTA

Introduction

Industrial solid wastes of different origin e.g. metallurgical wastes, ashes from power plants, wastes from smelting or melting operations etc., are used as raw materials in various industries [1, 2]. The steel mill pickling effluents are processed in two ways. The first is the acid regeneration process where the acids are recovered and reused. The size of the needed unit limits economically this process to large size steel works and in addition neutralization is also needed because 100% of regeneration is not achieved. In many smaller steel plants is used the second way, where the pickling effluents are neutralized by calcium hydroxide and then follows condensation in sedimentation tanks and disposal of the sludge either as it is, or in the form of cakes taken after dewatering by filter or vacuum press. In this way thousands of tones per year of iron containing solid wastes affect by their disposal the soil and water quality, represent a wastage in economic terms and additionally their administration becomes increasingly difficult the greater their bulk. The development of hematite after the thermal treatment of these wastes and the utilization of the product obtained, as red pigment for dolomite-concrete products, has been investigated in the past [3] and the suggested thermal transformation technique is already followed today [4]. Detailed work is needed in order: 1st to determine all the possible useful products that could be obtained out of these wastes, 2nd to design the proper production processes that could lead to different products, 3rd to

quantify the amounts of these useful products and 4th to present a techno-economical study that might suggest a relevant investment.

In the present work are studied the phase changes during thermal treatment of iron containing solid wastes of steel mill pickling lines by employing thermogravimetric (TG) and differential thermal analysis (DTA), Fourier transform infrared analysis (FTIR), as well as X-ray powder diffraction analysis (XRD) and atomic absorption spectroscopy (AAS) methods and it is expected to be a guide for the design of production processes for useful products that could be obtained.

Experimental

The iron containing wastes used in this study were produced due to cold rolling of hot rolled steel coils. The hot rolled steel coils follow the pickling process and continue to cold rolling in a tandem continuous cold rolling mill. Acidic effluents from pickling lines and effluents from tandem continuous cold rolling mill that contain emulsions, oils and iron in various forms (iron fines, iron soaps, etc.) are collected in a mixing tank where the pH is 5 to 5.5. The whole is transferred to a neutralization tank, calcium hydroxide is added and the pH value is increased to reach values between 9.5 and 10.5. After pH adjustment, is transferred to sedimentation tank, then to a thickener and finally to a vacuum drum filter. The wastes used in our study are the disposed in landfill sludge, from the pre-mentioned

* Presented at MEDICTA Conference 2005, Thessaloniki, peer reviewed paper.

** Author for correspondence: sikalidi@eng.auth.gr

drum filter and consist the main quantity of steel mill iron containing wastes. Samples of the wastes were collected, air-dried at room temperature, passed through a 40 mesh sieve and used for the experimental work. The chemical analyses of the wastes were performed using a PerkinElmer 503 Atomic Absorption Spectrometer. The analysis of the anions was performed by high-pressure liquid chromatography (Wescan ion chromatographic module). The particle size distribution analyses of the samples, was carried out using a Leeds Northrup microtrac particle size analyzer. In order to select the peak temperatures for the thermal treatment and to identify the critical temperatures, TG-DTA analyses were performed using a Setaram SETSYS 1750 TG-DTA system. Samples (32 ± 0.5 mg) were placed in alumina crucible. An empty alumina crucible was used as reference. Samples were heated from ambient temperature to 850°C , with heating rate $10^\circ\text{C min}^{-1}$, in static air. The FTIR spectra in the spectral area $4000\text{--}250\text{ cm}^{-1}$, were measured in a Bruker FTIR spectrometer, model IFS113v, in transmittance mode, with a resolution 2 cm^{-1} . X-ray diffraction analyses were performed, using a Siemens D500 X-ray diffractometer (λ_{Cu}).

The wastes were thermally treated at 275, 500, 700 and 850°C for 30 min in a Heraeus box type furnace, using a heating rate of $10^\circ\text{C min}^{-1}$. The samples then were cooled to room temperature by shutting off the furnace. The identification of the phases that are present in the samples, before and after their thermal treatment, was performed mainly by FTIR analyses. Additionally, X-ray diffraction measurements were used in order to verify our results. For the FTIR analyses the sample powders were mixed with CsI in order to produce pellets at about 0.8 mass/mass% of the sample.

Results and discussion

The determined particle size distribution of the wastes, showed a relatively fine dust (90 mass% $< 75.6\text{ }\mu\text{m}$, 50 mass% $< 10.58\text{ }\mu\text{m}$, 10 mass% $< 2.28\text{ }\mu\text{m}$). The results of chemical analysis of wastes before thermal treatment are given in Table 1. Chemical analysis showed that the main elements are iron, calcium and silicium while magnesium is contained only in a smaller quantity. In addition to inorganic, organic materials as iron soaps, emulsions and oils co-exist, in different percentages, affecting the loss on ignition (L.O.I.) values.

Combined use of the characterization methods of TG-DTA and FTIR enabled us to follow the phase changes during thermal treatment of these wastes.

In Fig. 1 are presented the heat flow and mass loss dependences on temperature for the initial waste prod-

Table 1 Chemical analysis of iron solid wastes before thermal treatment

Oxides	Mass%
Fe ₂ O ₃	46.7–49.8
CaO	16.8–19.7
MgO	2.2–2.7
Al ₂ O ₃	0.3–0.7
SiO ₂	4.6–5.9
L.O.I.	13.8–25.2
Cl ⁻	2.2–4.8
SO ₄ ²⁻	0.04

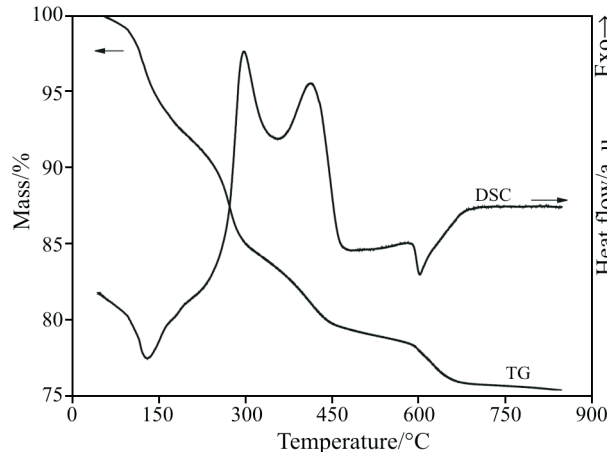


Fig. 1 DSC and TG curves of the initial material

ucts. The temperature-dependent mass loss of the wastes till 850°C , about 24.5 mass%, can be seen. As it is clear from the thermal curves there are four discrete temperature regions concerning to mass loss. These regions are: I) $80\text{--}180^\circ\text{C}$, II) $180\text{--}325^\circ\text{C}$, III) $325\text{--}485^\circ\text{C}$ and IV) $555\text{--}710^\circ\text{C}$. In the DSC curve we follow two endothermic and two exothermic peaks were found. The two exothermic peaks correspond to the (II) and (III) steps of mass loss, while the two endothermic to the (I) and (IV) steps.

The thermal curves give us the possibility to select the appropriate specific temperatures for the heat treatment procedure. The products heated at that temperatures are characterized by FTIR, X-ray methods and thus follow the successive phase changes of the initial material.

Initial material

The variety of the components that co-exist in the initial material is reflected in the initial FTIR spectrum (Fig. 2). The presence of the calcite (CaCO_3) is clear from three characteristic peaks of the calcite's carbonate ($1475\text{--}1420$, 870 and 713 cm^{-1}). The weak broad band at the spectral area $1200\text{--}1130\text{ cm}^{-1}$, which remains un-

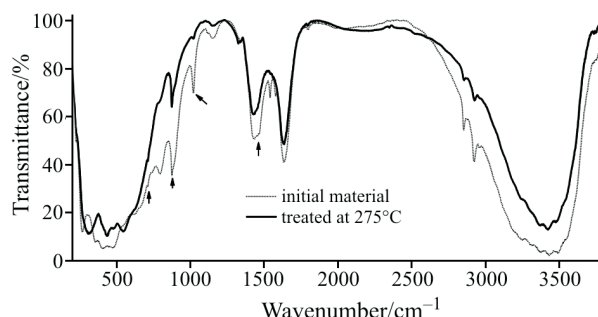


Fig. 2 FTIR spectra of the initial and thermally treated (at 275°C) material

changeable during the total thermal treatment, is an indication for the presence of quartz as trace material. Moreover the weak sharp peaks at 2956, 2923, 2855, 1577 and 1540 cm^{-1} suggest the existence of organic phase(s) in small quantities as a result of the treatment line.

As far as it concerns the iron containing components, lepidocrocite ($\gamma\text{-FeOOH}$) is identified as the main iron component by the peaks at 1020 and 750 cm^{-1} , which are attributed to OH stretching and Fe–O bending vibrations, respectively. Also, could be identified small participation of I) goethite ($\alpha\text{-FeOOH}$) due to the presence of a shoulder at $\sim 885 \text{ cm}^{-1}$ and II) amorphous $\delta\text{-FeOOH}$ due to the presence of broad peaks at 1124 and 790 cm^{-1} [5, 6]. Finally the spectral area above 700 cm^{-1} – which characterizes mostly the Fe–O vibrations – presents a very broad band making difficult an unambiguous assignment. The above findings are supported from the XRD analysis of the initial product.

Heat treatment at 275°C

Following the changes due to the thermal treatment, the spectra from the thermal treated material at 275°C and the initial (Fig. 2) are compared and we can comment for the peaks: I) $\gamma\text{-FeOOH}$ and $\delta\text{-FeOOH}$ almost disappear, II) $\beta\text{-FeOOH}$ is present with a decreased intensity and therefore, participation, III) peaks due to organic groups almost disappear, IV) calcite and quartz remain unchangeable.

Additionally, the broad band below 700 cm^{-1} begins to be resolved and we can observe a shoulder at 630 cm^{-1} and three peaks at about 550, 430 and 310 cm^{-1} [7–9]. These characteristics (especially the shoulder at 630 cm^{-1}) are indication for the presence of iron oxide phases with a spinel structure, but with low crystallinity. This phase is identified as maghemite ($\gamma\text{-Fe}_2\text{O}_3$) which is formed from $\gamma\text{-FeOOH} \rightarrow (\gamma\text{-Fe}_2\text{O}_3)$ [6, 10, 11].

Heat treatment at 500°C

The spectrum of the sample treated at 500°C (Fig. 3) – beyond the bands of the calcite and quartz – in the area below 700 cm^{-1} presents the same band arrangement with the treated at 275°C, the only difference being that the bands are now well resolved and the shoulder at about 630 cm^{-1} has a better definition. This well-resolved absorption bands were due to the ordered spinel structure ($\gamma\text{-Fe}_2\text{O}_3$), which exhibits a larger number of IR bands than the disordered material [7, 8]. The appearance of a weak shoulder at about 475 cm^{-1} is indicative of the presence of hematite ($\alpha\text{-Fe}_2\text{O}_3$) due to the conversion of the small amount of goethite.

Heat treatment at 700°C

Multicomponent bands in Fe–O vibration area (700–300 cm^{-1}) are also shown in the spectra of the studied material after heating at 700°C (Fig. 3) but there

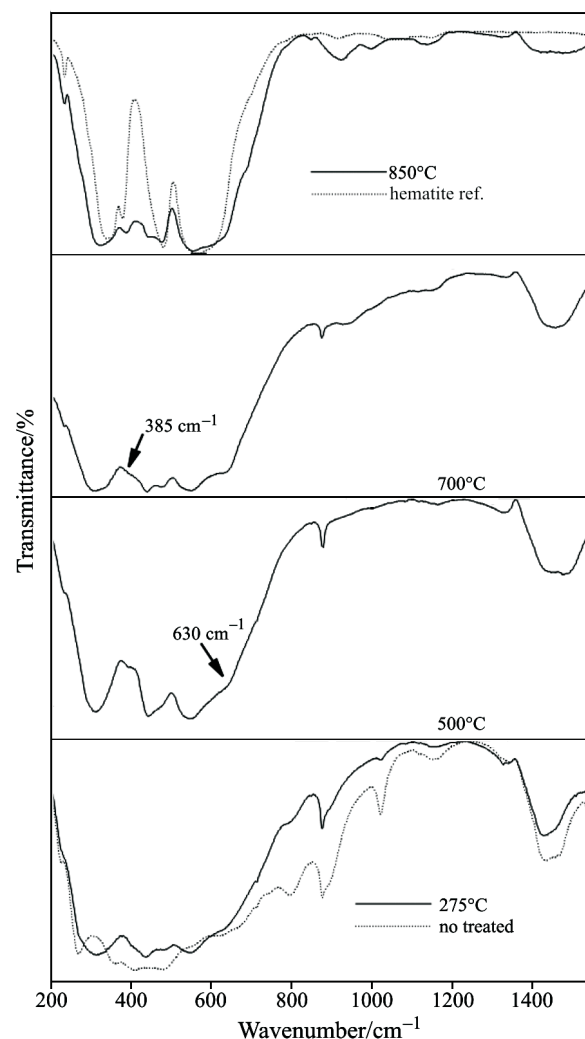


Fig. 3 FTIR spectra of the initial and the thermally treated material at 275, 500, 700 and 850°C

are some differences at the maximum frequencies and relative intensities for each one. This is an indication that a structural transformation took place. The clear presence of 475 cm^{-1} band and a weak shoulder at 385 cm^{-1} leads to the conclusion that during the thermal treatment at 700°C a part of maghemite is converted to hematite, and thus in the final material we follow the co-existence of maghemite and hematite as a mixture.

Heat treatment at 850°C

Increasing the maximum heat treatment temperature, the percentage of maghemite is decreased through its transformation to hematite. Above 850°C , as it can be seen from the FTIR spectra (Fig. 3), the calcite has almost been decarbonated and hematite is the main constituent with a small participation of maghemite. A part of the remaining CaO probably forms with Fe_2O_3 , calcium ferrites ($\text{Ca}_4\text{Fe}_{14}\text{O}_{25}$, or CaFe_2O_4).

Integrating the analysis of phase changes observed in the thermal plot, through FTIR spectra, the peaks in the diagrams of Fig. 1 can be attributed to their corresponding phase transformations. The amount of the absorbed water drives off in temperatures ranging from $80\text{--}160^\circ\text{C}$ (first step of mass loss). The second step of mass loss corresponds to the decomposition of $\gamma\text{-FeOOH}$ and is followed by the formation of $\gamma\text{-Fe}_2\text{O}_3$ [12–14]. In the same temperature region is recorded and the elimination of the organic phases, as the first exotherm peak in the DSC curve. The main phase transformation of γ - to $\alpha\text{-Fe}_2\text{O}_3$ takes place at the second exothermic peak. At the same temperatures are found and the changes in $\alpha\text{-FeOOH}$. The third exothermic peak in the DSC curve is due to $\alpha\text{-FeOOH}$ decomposition [15] and the formation of $\alpha\text{-Fe}_2\text{O}_3$. As the quantities of $\alpha\text{-FeOOH}$ and $\delta\text{-FeOOH}$ are relatively small and their transformations take place in the same – more or less – temperature region, these phase changes are not well visible in the DSC curve. The fourth mass loss step indicates the decomposition of calcite and the CO_2 removal. The XRD results are in good agreement with those from FTIR giving additionally more specific results about the presence of calcium iron oxide (Fig. 4).

Summarizing the obtained results we can say that lepidocrocite remains in small quantities till heating at 275°C . At higher temperatures, the thermally treated powders contain a mixture of $\alpha\text{-Fe}_2\text{O}_3$ (hematite) and $\gamma\text{-Fe}_2\text{O}_3$ (maghemite) in different proportions [2, 3], depending on the maximum heating temperature of the thermal treatment. Increasing the maximum temperature the dominant participation of maghemite ($\gamma\text{-Fe}_2\text{O}_3$, brown pigment) is decreased through its transformation to hematite ($\alpha\text{-Fe}_2\text{O}_3$, red pigment). Hematite (red iron pigment) is a very important commercial product. Calcite is present till at 750°C while follows the de-

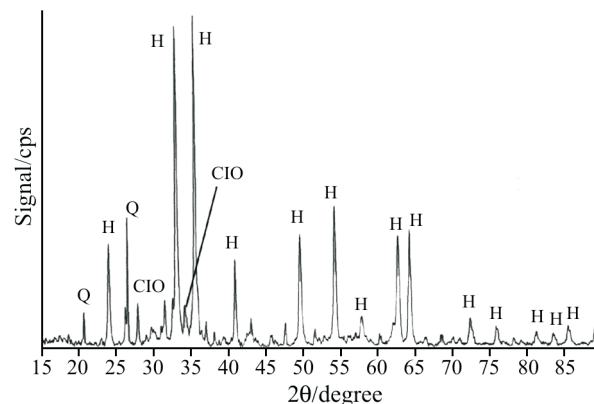


Fig. 4 X-ray diffractograms of iron solid wastes after their thermal treatment at 850°C . H=hematite, CIO=calcium ferrites, Q=quartz

composition process. In case of high content of CaCO_3 and in the case of thermal treatment that will favor it, calcium iron oxide might appear. The decomposition product of calcite is lime (CaO). Calcium ferrite was the result of the solid-state reaction between CaO and Fe_2O_3 . Even before the temperature of 700°C , calcium oxide generated from the decomposition of CaCO_3 , reacts with iron phases giving calcium ferrites ($\text{Ca}_4\text{Fe}_{14}\text{O}_{25}$, or CaFe_2O_4) [16] that are characteristically identified in the XRD patterns (Fig. 4). The presence of calcium compounds is undesirable in the final product because it affects the tinting strength of the pigment. Using hydrated lime for neutralization of the wastes without calcite, the problem of undesirable calcium compounds will be solved. Better results could be obtained by washing the wastes after the drum filter. In addition, more care in handling of the wastes will eliminate also the presence of undesired quartz e.g. the washed wastes could be transported directly to a rotary kiln for thermal treatment. In temperatures above 850°C hematite is the main constituent. X-ray semi-quantitative mineralogical analysis showed that after 30 min at 850°C the presence of hematite ($\alpha\text{-Fe}_2\text{O}_3$) was around 45 mass%. The temperature of 850°C was also chosen in order to achieve the complete decomposition of calcite that exists in the wastes. Although the percentage of hematite is relatively low, the tinting power of this not upgraded product, was found to be adequate for utilization as pigment for certain products [1]. Upgraded wastes without calcium compounds and quartz, could give after thermal treatment a red iron pigment with very high hematite content and hence very high tinting power, which would have broader applications.

Conclusions

The phase changes during thermal treatment of iron containing solid wastes of steel mill pickling lines were mainly described by means of DSC, TG and FTIR. Above 275°C, the thermally treated wastes contain a mixture of $\alpha\text{-Fe}_2\text{O}_3$ (hematite) and $\gamma\text{-Fe}_2\text{O}_3$ (maghemite) in different proportions, depending on the maximum heating temperature of the thermal treatment. Increasing the maximum temperature the maghemite participation is decreased through its transformation to hematite. A red pigment based on hematite can be obtained after thermal treatment at 850°C. The proper production processes could lead to different products with regard to their final properties.

References

- 1 C. Sikalidis, *Fresenius Environ. Bull.*, 8 (1999) 457.
- 2 S. Meillon, H. Dammak, E. Flavin and H. Pascard, *Philosophical Letters*, 72 (1995) 105.
- 3 R. M. Cornell and U. Schwertmann, *The iron oxides: structure, properties, reactions occurrence and uses*, VCH, (1995).
- 4 N. E. Fouad, H. M. Ismail and M. I. Zaki, *J. Mater. Sci. Lett.*, 17 (1998) 27.
- 5 Y. Wan, C. Yan, J. Tan, Z. Shi and C. Cao, *J. Mater. Sci.*, 38 (2003) 3597.
- 6 K. S. Rane, V. M. S. Verenkar and P. Y. Sawant, *Bull. Mater. Sci.*, 24 (2001) 331.
- 7 M. C. Blesa, E. Morán, J. D. Tornero, N. Menentez, E. Mata-Zamora and J. M. Saniger, *J. Mater. Chem.*, 9 (1999) 227.
- 8 T. Belin, N. Guigue-Millot, T. Caillot, D. Aymes and J. C. Niepce, *J. Solid State Chem.*, 163 (2002) 459.
- 9 A. A. Khaleel, *Chem. Eur. J.*, 10 (2004) 925.
- 10 R. V. Morris, H. V. Lauer Jr., C. A. Lawson, E. K. Gibson Jr., G. A. Nace and C. Stewart, *J. Geophys. Res.*, 90 (1985) 3126.
- 11 S. Ponce-Castaneda, J. R. Martinez, S. Palomares-Sanchez, F. Ruiz, O. Ayala-Valenzuela and J. A. Matutes-Aquino, *J. Sol-Gel Sci. Technol.*, 27 (2003) 247.
- 12 F. S. Yen, W. C. Chen, J. M. Yang and C. T. Hong, *Nano-Letters*, 2 (2002) 245.
- 13 I. Mitov, D. Paneva and B. Kunev, *Thermochim. Acta*, 386 (2002) 179.
- 14 A. R. Dinesen, C. T. Pedersen and C. Bender Koch, *J. Therm. Anal. Cal.*, 64 (2001) 1303.
- 15 R. L. Frost, Z. Ding and H. D. Ruan, *J. Therm. Anal. Cal.*, 71 (2003) 783.
- 16 B. S. Randhawa, K. J. Sweety, M. Kaur and J. M. Greeneche, *J. Therm. Anal. Cal.*, 75 (2004) 101.

Received: August 1, 2005

Accepted: November 21, 2005

OnlineFirst: June 27, 2006

DOI: 10.1007/s10973-005-7168-8